Journal of ELECTRONIC MATERIALS, Vol. 46, No. 7, 2017
DOI: 10.1007/s11664-017-5464-2
© 2017 The Minerals, Metals & Materials Society

CrossMark

Die Bonding Performance Using Bimodal Cu Particle Paste Under Different Sintering Atmospheres

YUE GAO,[1,2] HAO ZHANG,[1] WANLI LI,[1] JINTING JIU,[1,3] SHIJO NAGAO,[1] TOHRU SUGAHARA,[1] and KATSUAKI SUGANUMA[1]

1.—The Institute of Scientific and Industrial Research (ISIR), Osaka University, Mihogaoka 8-1, Ibaraki, Osaka 567-0047, Japan. 2.—e-mail: gao.yue@eco.sanken.osaka-u.ac.jp. 3.—e-mail: jiu@eco.sanken.osaka-u.ac.jp

A one-step polyol method was employed to synthesize bimodal Cu particles with average diameters around 200 nm and 1000 nm, respectively. The bimodal Cu particles were mixed with a reductive solvent of polyethylene glycol (PEG) to form a paste. The Cu paste was used as die bonding material to prepare Cu joints under N_2 or vacuum sintering atmosphere. The results showed that the strength of the Cu joints in N_2 atmosphere was always higher than that in vacuum. The shear strength of a Cu joint processed at 350°C under only 0.4 MPa bonding pressure in N_2 was above 40 MPa, which was far higher than that obtained using single-sized nano-Cu particle paste. It is related to the dense packing of the bimodal Cu particles and slow decomposition behavior of the reductive PEG solvent. The reductive PEG solvent in the Cu paste, which effectively removed oxides on the surface of the Cu particles, was necessary for easy-oxidized Cu pastes. These results suggested that Cu pastes with suitable particle sizes, reducing solvent and sintering atmosphere could be a proper candidate for low-temperature and low-pressure bonding process.

Key words: Bimodal Cu particles, sintering atmosphere, polyethylene glycol, die-attach materials, shear strength

INTRODUCTION

The application of wide band gap (WBG) semiconductor materials like silicon carbide (SiC) or gallium nitride (GaN) in high-power devices is considered to be a revolution of the traditional semiconductor industry because these WBG semiconductors can withstand harsher environments such as high temperature, high current density, severe thermal shocks and high frequency.[1,2] However, traditional die bonding materials would break down at high temperatures hindering the development of WBG semiconductors. Thus, it is vital to search for novel die-attach materials which can not only bond SiC/GaN to substrates but also endure high working temperatures and high-frequency thermal shocks before WBG devices can enter the market.[3,4] Die-attach materials based on metallic nanoparticles have been proved to be promising alternatives due to their low processing temperature and high working temperature. For example, Ag joints formed with Ag nanoparticle (Ag-NPs) paste have high electrical/thermal conductivity and also show excellent stability of shear strength even with high temperature and thermal shock tests.[5–7] However, Ag is expensive and susceptible to electromigration, which will readily induce short circuits or open circuits between joints, especially in mainstream fine-pitch packages.[8]

Cu paste is expected to be a potential substitute for Ag paste because Cu is only 6% less conductive than Ag, but 100 times less expensive.[9,10] In addition, Cu is more robust against electromigration.[11] Hence, Cu nanoparticle (Cu-NP) pastes as die-attach materials have attracted increasing attention.[12,13] However, Cu is easily oxidized in air even at room temperature, especially for Cu-NPs. The bonding processing of Cu-NPs pastes becomes difficult and complicated in order to remove Cu oxides

(Received October 3, 2016; accepted March 17, 2017; published online March 27, 2017)

on the surface of Cu-NPs. The bonding procedure using Cu-NP paste always refers to a reductive atmosphere (such as in H_2, formic acid) and high temperature.[14,15] Solvents used in the paste are an important factor, which influence the sintering process and the final quality of the bonding joints.[16–19] Considering the oxidation issue of Cu particles, a solvent with reducibility should be suitable and helpful for the removal of Cu oxides. For example, polyethylene glycol (PEG) was used to remove the oxide layer on Cu chips to make direct contact with the Ag paste under high pressure and high temperature.[25] Ogura et al. directly used CuO and Ag_2O nanoparticle paste with PEG solvent to make Cu-Cu joints at 300°C, during which both Ag_2O and CuO were reduced to pure metal by PEG even in air.[20,21] These results suggested that PEG was a suitable solvent to make Cu-NP paste without a reductive atmosphere. Furthermore, the decomposition process of PEG solvent would be affected by the sintering atmosphere; unfortunately, studies seldom focus on this point.

The size of the Cu-NPs is another key factor in Cu paste. Small Cu-NPs melted at lower temperature were more easily oxidized compared with larger Cu particles. To achieve balance, bimodal Cu paste based on mixed Cu particles with different sizes may be a promising solution by decreasing both the content of the Cu oxides and the melting temperature of the Cu paste. Bimodal Ag pastes have been proved to be successful to achieve metal joints with high bonding strength,[2,22,23] excellent electrical conductivity and thermal stability.[6,24] Based on this inspiration, some bimodal Cu pastes have been developed. Kim et al. used intense pulse light to sinter a Cu paste composed of large particles of 2 μm and small particles of 20–50 nm in diameter and achieved a dense Cu pattern with a low resistivity of 80 $\mu\Omega$ cm. The value was lower than that obtained with mere Cu-NPs or mere micron Cu.[25] They suggested that the Cu-NPs played a nano-welder role and enhanced the connection between the Cu microparticles. Tam et al. also mixed 9.3-μm Cu flakes and 60.8-nm Cu particles to get a Cu pattern with a low resistivity of 28 $\mu\Omega$ cm. The Cu-NPs first melted and then fused during sintering which provided the interconnection among the Cu flakes and improved the electrical conduction.[26] These results indicated that, besides the low content of oxides and low melting temperature, the bimodal Cu paste also showed superiority in obtaining dense bonding joints, which is important to achieve high strength and high reliability. These merits of the bimodal Cu paste stimulated us to design suitable Cu pastes by optimizing the size distribution of the Cu particles.

Here, bimodal Cu particles containing two sizes of particles were synthesized by a simple, large-scale polyol method, as set out in our previous paper.[27] The bimodal Cu particles were mixed with PEG solvent to make pa aste for the die bonding process. Cu joints were realized in both N_2 and vacuum atmospheres. The thermal properties of the Cu bimodal pastes were measured. The microstructure and shear strength of the Cu joints were examined. The detailed mechanism will be discussed in the following sections.

EXPERIMENTAL

Synthesis of Bimodal Cu Particles

A modified polyol method was used to prepare bimodal Cu particles,[27] in which 1.5 g Polyvinyl Pyrrolidone K90 (PVP) as capping agent and dispersant was first dissolved into 1,3-propanediol (PDO). Then, 1.5 g copper hydroxide ($Cu(OH)_2$) was dissolved in the above solution at room temperature. After that, the solution was immediately heated to 190°C and reacted for about 90 min. Then, the dark red precipitation was immediately centrifuged and washed several times to get pure Cu particles, and finally these particles were kept in ethanol for further use.

Fabrication of Cu Joints

The as-synthesized bimodal Cu particles were mixed with PEG (PEG300) with a mass ratio of 1:0.15 to form the Cu paste. The paste was screen-printed on a Cu substrate by a stainless steel screen (4 mm $\times$ 4 mm $\times$ 0.1 mm), and then a Cu chip (4 mm $\times$ 4 mm $\times$ 0.8 mm) was placed on the surface of the paste layer. After drying in air for several minutes, the joints were sintered in a vacuum environment or a N_2 atmosphere with a bonding pressure of 0.4 MPa. The sintering process in the N_2 atmosphere was carried out in a solder re-flow sintering system (RSS-210; UniTemp) with a N_2 flow rate of 1 L/min. The vacuum condition was created by a fine vacuum system (YONEKURA). In both conditions, the heating rate was 25°C/min.

Characterization and Properties

The phase of the Cu particles was checked by x-ray diffraction (XRD; RINT 2500; Rigaku) and x-ray photoelectron spectroscopy (XPS; JPS-9010MC; JEOL). The morphology of the Cu particles and the microstructure of the Cu joints were examined by a field emission scanning electron microscope (FE-SEM; SU8020; Hitachi). Thermogravimetry differential thermal analysis (TG–DTA; STA449 F3; NETZSCH) was used to analyze the thermodynamic behavior of the Cu paste and the reductive solvent of PEG. Cross-section samples were fabricated by an ion-milling process (IM4000; Hitachi). The mechanical property of the metallic Cu joint was evaluated by a shear test (XD7500; DAGE) with a shear strain rate of 1 mm/min.

RESULTS AND DISCUSSION

Figure 1a shows the XRD pattern of the Cu product. There are three main characteristic peaks

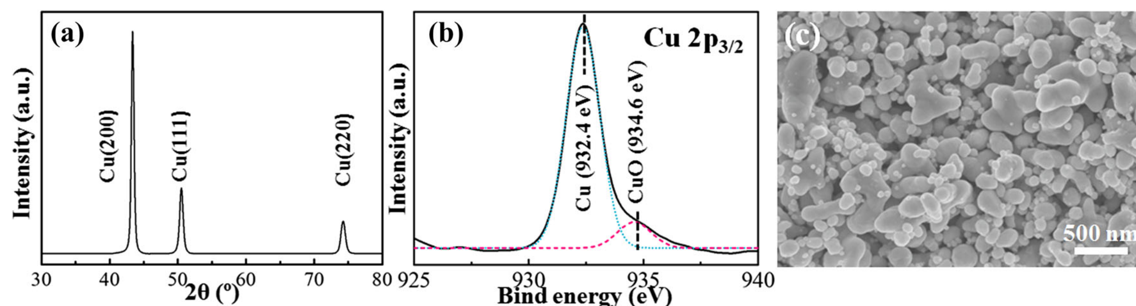

Fig. 1. XRD pattern (a), XPS spectra (b) and FE-SEM micrograph (c) of as-synthesized Cu particles.

located at $2\theta = 43.3°$, 50.4°, and 74.08°, which correspond to the diffraction of the (111), (200), and (220) planes of the face-centered cubic (fcc) Cu crystal, respectively.[28] No other impurity phases such as CuO, Cu_2O, or $Cu(OH)_2$ were observed. However, the XPS measurement indicated the existence of Cu oxides, which might partly cover the surface of the Cu particles (Fig. 1b). In the spectrum of Cu $2p_{3/2}$, a peak at 934.3 eV corresponds to the Cu oxides. The existence of Cu oxides was due to the intrinsic easy oxidization of Cu even in ambient atmosphere.[29] Since the melting temperature of the Cu oxides was extremely high, their existence would obstruct the connection of the Cu particles. Figure 1c shows the SEM micrographs of the as-synthesized Cu particles. It can be clearly observed that the size of the Cu particles was extremely non-uniform including small and large particles, which had a wide size distribution from nanoscale to microscale. While most small particles had an average diameter of 200 nm, the large particles had an average diameter of 1000 nm. In addition, the morphology of the small and large particles were different. The small particles tended to be round-shaped and the large particles had a rod-like irregular appearance. This indicated that bimodal Cu particles were successfully prepared using the simple, one-pot polyol method.

The bimodal Cu particles were mixed with PEG and used to die-bond Cu chips under a low bonding pressure of 0.4 MPa. To test the bonding strength of the Cu paste, the shear strength was examined as the bonding strength of the Cu joints. Figure 2 shows the shear strength of the Cu joints under N_2 and vacuum atmospheres compared with other results. It is clear that the shear strength of these Cu joints was always increased when the bonding temperature increased in all the groups. In vacuum condition, the shear strengths of the Cu joints were 10.1 MPa, 15.4 MPa and 21.6 MPa when the bonding temperatures were 250°C, 300°C, and 350°C, respectively. Higher strengths of 13.1 MPa, 22.4 MPa and 40.6 MPa were obtained in the same conditions in the N_2 atmosphere. The shear strengths obtained by present bimodal particle paste were much higher than those of the Cu-NPs pastes. Nishikawa et al. bonded Cu chips by Cu-NP

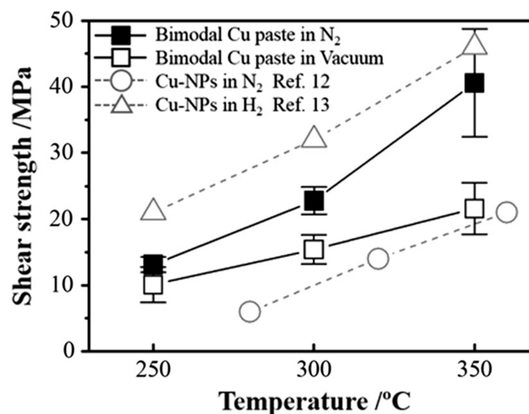

Fig. 2. Shear strength of Cu joints of the bimodal Cu paste. Experimental condition: particle size: 10–20 nm, pressure: 15 MPa in Ref. 12; particle size: 20–94.4 nm pressure: 5 MPa in Ref. 13.

(10–20 nm) paste in a glycol solvent under a pressure of 5 MPa at 360°C in a N_2 atmosphere. The shear strength of the as-prepared joint was only 20 MPa.[12] Although a higher shear strength of 40 MPa was achieved at 350°C using Cu-NPs (20–94.4 nm) paste, a complex two-step sintering process in reductive H_2 gas was necessary to remove the oxide layer on the surface of the Cu-NPs.[13] These results proved that the bimodal Cu bimodal paste presented in this work was a powerful alternative compared with those Cu-NPs pastes. On the other hand, it should be noted that an obvious discrimination in strength under different atmospheres was observed, which might be related to the decomposition behavior of PEG in the Cu paste. This will be discussed later.

Figure 3 shows the SEM micrographs of the fracture surface of the Cu joints. It can be seenthat small Cu particles were filling the interspace between the large Cu particles, and thus dense packaging structures were achieved after the sintering process. At the relatively low temperature of 250°C, the Cu particles almost kept the initial morphology regardless of the sintering atmosphere (Fig. 3a and d). When the bonding temperature rose to 300°C, obvious necking growth arose to join the small particles into larger particles. The grain size of the joint formed in the N_2 atmosphere was almost

twice that in vacuum (Fig. 3b and e), which resulted in the high shear strength of the Cu joints in N_2, as shown in Fig. 2. However, there were still many isolated Cu particles. When the bonding temperature was increased to 350°C, a bulk-like Cu joint was realized in N_2 atmosphere without any individual small Cu particles (Fig. 3f). On the other hand, in the case of the vacuum atmosphere, individual Cu particles still existed in the joint (Fig. 3c). It is interesting to find that the isolated particles were smaller than 200 nm. Generally, smaller particles were easier to melt compared to the larger ones, but here the opposite result was observed. This abnormal behavior was possibly because the oxide layer on the surface of the small Cu particles, which was confirmed by the XPS results (Fig. 1b), hindered the sintering of the small Cu particles.

Figure 4 shows cross-section micrographs of Cu joints in vacuum and N2 atmosphere. Dense microstructures were obtained with increasing the sintering temperature in both cases. At 250°C, a close-packed structure was observed owing to the matching effect of the bimodal Cu particles. However, these Cu particles existed individually with clear boundaries between them. The interface between the paste and substrates was also clearly distinguishable (Fig. 4a and d). At 300°C, clear neck-growth and network structure was observed. The small particles were seen to connect to large particles as bridges. However, there were still some individual Cu particles in the voids of the Cu paste. The interface of paste and substrate was also different. It seemed that Cu particles fused into the Cu substrate to make full contact between the

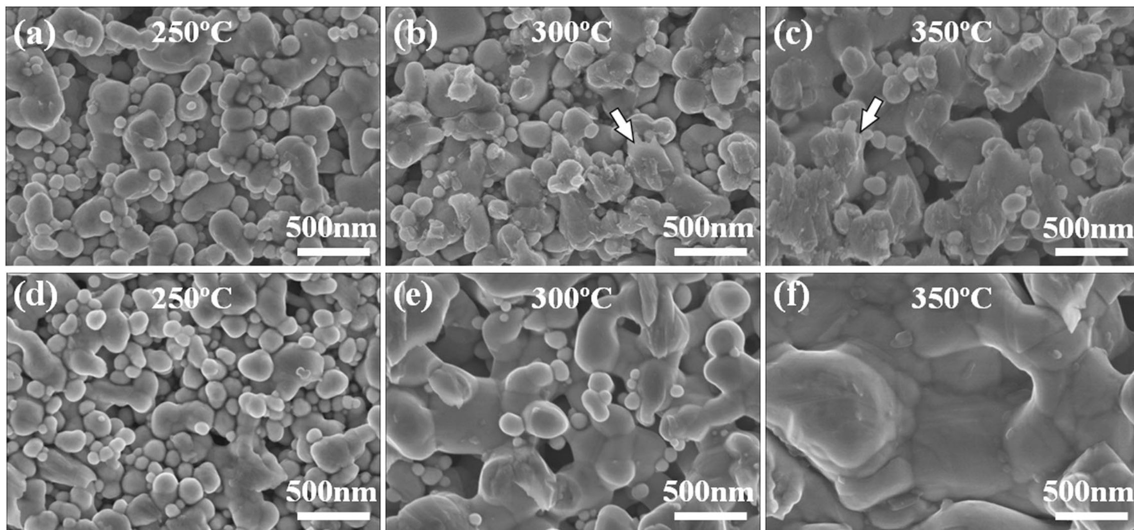

Fig. 3. FE-SEM micrographs of the fracture surface of the Cu joints under vacuum (a–c) and N_2 (d–f) at different temperatures.

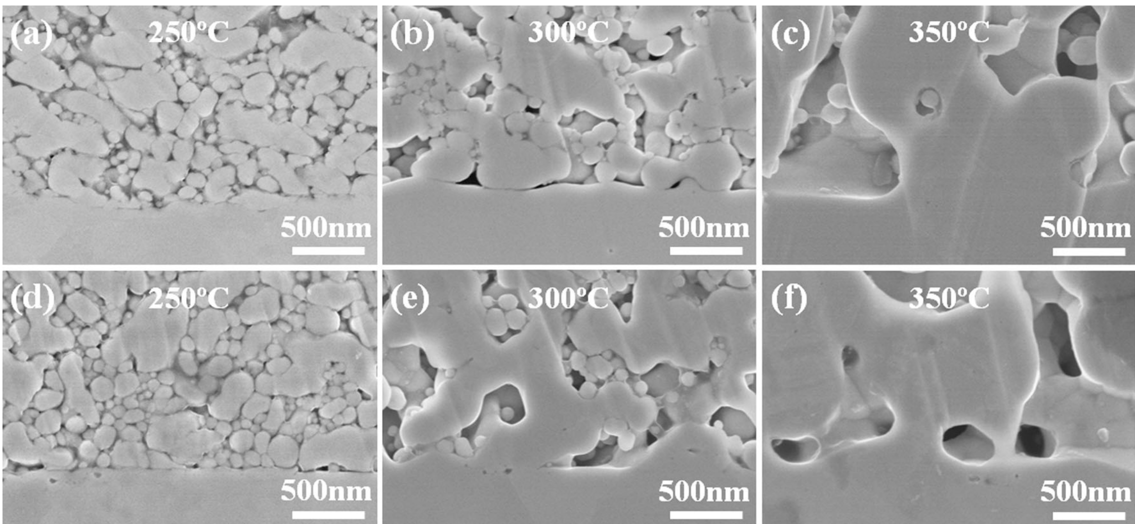

Fig. 4. FE-SEM micrographs of the cross-section of Cu joints under vacuum (a–c) and N_2 (d–f) bonded at different temperatures.

paste and substrate in the N_2 atmosphere (Fig. 4e). In contrast, the clear distinction between the Cu paste and substrate was still seen in vacuum (Fig. 4b). As the bonding temperature rose to 350°C, the Cu paste was fully fused into the Cu substrates without a clear interface line in either case, which led to improved strength. Moreover, the isolated particles in the joint completely disappeared in the case of the N_2 atmosphere (Fig. 4f), but there were still some small particles in the joint in the case of the vacuum (Fig. 4c). The existence of these isolated small particles might cause defective voids in the joint leading to lower strength compared with that sintered in N_2.

Thermal analysis is used to clarify the difference in vacuum and N_2 atmosphere. Figure 5 shows the TG–DTA curves of related samples. An exothermic peak around 250°C was observed with corresponding weight-loss when the Cu pastes were sintered in both vacuum and N_2 atmosphere (Fig. 5a and b). Generally, an exothermic peak in paste is usually related to the decomposition/combustion of organics. However, no similar peak was detected when pure PEG was heated in the same conditions (Fig. 5c and d). Instead, a small endothermic valley in N_2 and a large valley in vacuum was found with a significant weight loss. The endothermic valley corresponded to the evaporation of PEG. In order to pursue the reason for the large exothermic peak in the pastes, a CuO–PEG mixture with mass ratio of 1:0.15 was heated in N_2 (Fig. 5e). Interestingly, a similar exothermic peak was observed at around 240–290°C with a very strong peak, which contributed to the reduction of CuO into metal Cu by PEG.[21] In the present Cu paste, the existence of trace Cu oxides on the surface of the bimodal Cu particles was observed, as mentioned above. The PEG solvent must reduce these oxides into metal Cu during sintering, which gave a clear exothermic peak. On the other hand, comparing the weight-loss curves of the paste in the two cases, a rapid weight loss was observed at the related low-temperature range from 100 to 280°C in vacuum (Fig. 5b) while the weight-loss temperature was extended to 380°C in the N_2 atmosphere. Although PEG can reduce CuO to metal Cu,[21] the rapid and complete evaporation of PEG might cause an insufficient reduction of oxides in vacuum, which corresponded to the existence of small particles even at high temperature (Fig. 3c). In contrast, the slow and continuous release of PEG in N_2 up to 380°C ensured the totally removal of the oxides and promoted the sintering. This suggested that the decomposition behavior of the solvent in the Cu paste played an important role in the sintering process of the readily oxidized Cu particles.

To further confirm the reducing capacity of PEG, the bimodal Cu paste was deliberately aged in air until a detectable oxides peak was observed by XRD. Then, the paste was used to make bonded Cu chips. The shear strengths of the joints bonded with the aged Cu paste was compared with that of newly prepared Cu paste as shown in Fig. 6a. The strength of the Cu joints increased when the sintering temperature was elevated. Moreover, the strength of the joints using the aged Cu paste was lower than that using fresh Cu paste when processed at 250°C and 300°C. An almost equivalent shear strength of an average 38.1 MPa was obtained when the bonding temperature rose to 350°C for both pastes. Corresponding XRD patterns are shown in Fig. 6b. The aged paste gave a clear CuO peak, which disappeared after being sintered at 350°C. This result confirmed that the PEG effectively reduced Cu oxides on the surface of Cu

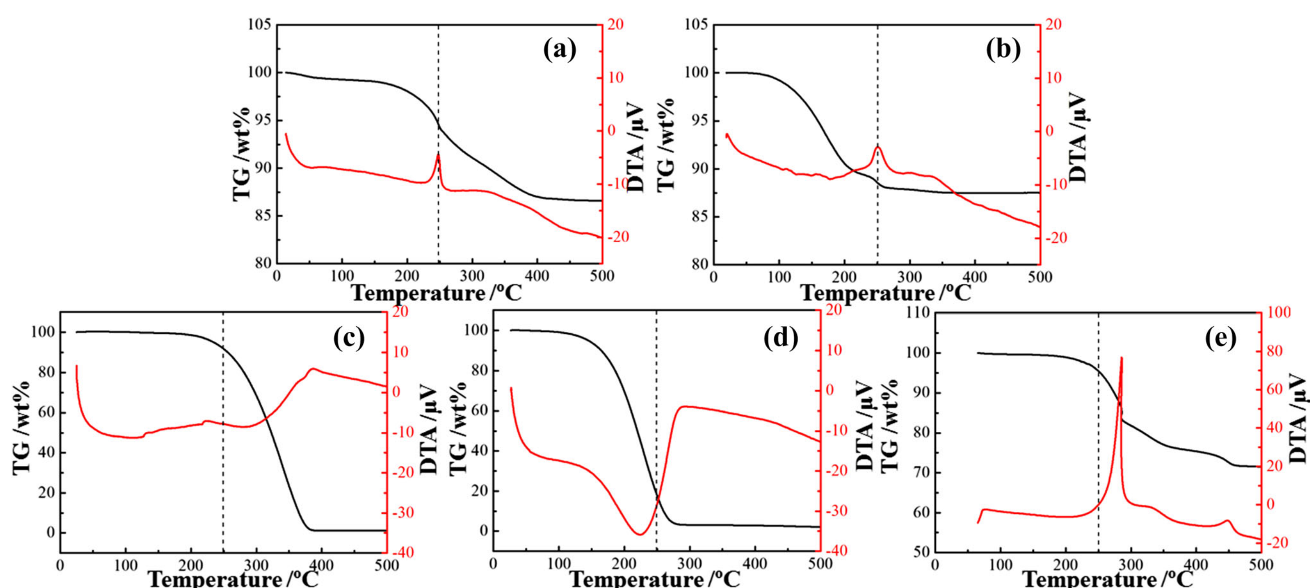

Fig. 5. TG-DTA of bimodal Cu paste sintered in N_2 (a) and vacuum (b), pure PEG solvent in N_2 (c) and vacuum (d), and the CuO–PEG mixture in N_2 (e).

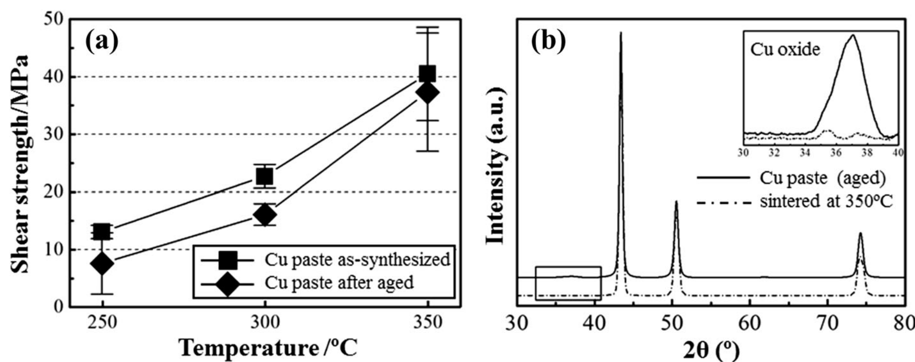

Fig. 6. Shear strengths (a) and XRD patterns before and after sintering in N_2 (b) of bimodal Cu paste aged in air. (Inset enlarged XRD pattern in the range of 30°–40°).

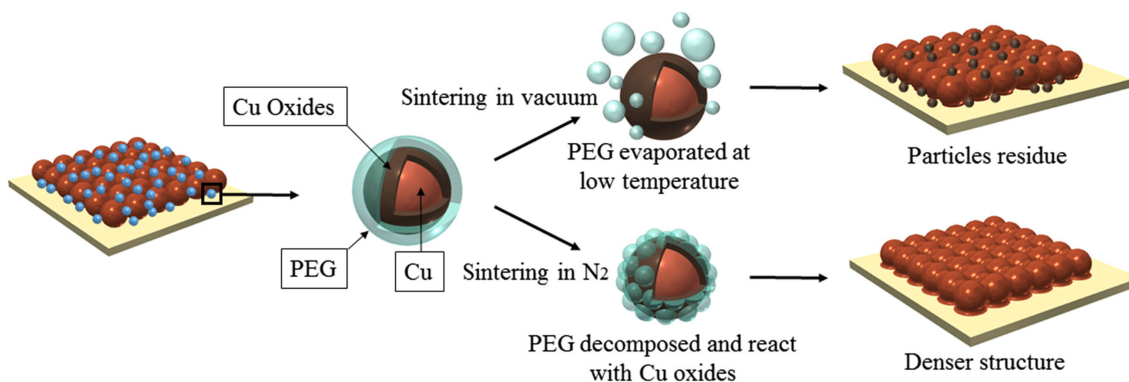

Fig. 7. Sintering mechanism of bimodal Cu paste in different atmospheres.

particles and promoted the strength of Cu joints sintered.in N_2 atmosphere when the sintering temperature is over 300°C. These results coincide with those reports about the reduction of PEG.[21] The joints bonded with aged Cu paste had a lower strength than that using fresh Cu paste at low sintering temperatures, which implied that optimizing the decomposition behavior of PEG in a sintering atmosphere played a main role. A suitable reductive solvent with proper decomposition behavior was a key factor for the sintering of easily oxidized Cu paste. The intrinsic easy oxidization of Cu determines the inevitable existence of oxides during synthesis, washing, storage and subsequent applications, and therefore a reductive solvent is necessary for Cu paste.

A possible mechanism for sintering behavior in different atmospheres is shown in Fig. 7. During fabrication of the paste, the small particles in the paste were partly oxidized to form a partial oxide shell, and large particles remained without oxidation. When the bimodal Cu paste was sintered, a dense structure was formed due to the matching of the bimodal particles. And then large particles were fused together by neck growth to make a network structure (Figs. 3 and 4). These small particles with the oxide shell filled in the spaces of the large particles. With the increase of sintering temperature, the PEG decomposed and reacted with the thin oxide shell on the surface of these small Cu particles and induced the neck growth for the formation of a bulk-like structure. In vacuum, the PEG was rapidly evaporated at low temperature and lost its reducing ability, resulting in a microstructure including isolated small Cu particles (Fig. 4). This induced defects and voids in the joints and caused a low strength. In the N_2 atmosphere, the PEG was slowly and continuously released to completely remove those oxides on the surface of the small Cu particles to make a dense Cu structure without remnant isolated Cu particles (Fig. 4), which contributes to the high bonding strength. This mechanism suggests that the choice of solvent and Cu particles with relative sintering atmosphere is important for the sintering of Cu particles under low temperature and low bonding pressure.

CONCLUSION

A one-step polyol method was developed to synthesize bimodal Cu particles. The as-synthesized bimodal Cu product included two sizes of particles with average diameters around 200 nm and 1000 nm, respectively. The bimodal Cu particles were utilized as die-attached materials to prepare Cu joints with a dense packing structure. The strength of the Cu joints depended on the sintering atmosphere and temperature. A high shear strength

of 40 MPa was obtained with a very low bonding pressure of 0.4 MPa at 350°C in a N_2 atmosphere. A vacuum atmosphere gave a strength of only 22.4 MPa in the same conditions. The reductive solvent was also necessary to remove the oxides in the Cu paste. The continuous decomposition behavior of PEG in the N_2 atmosphere produced joining between the Cu particles by removing oxides on their surface. A bimodal Cu particle paste combining a suitable reductive solvent provides a new way to produce high-performance Cu joints at a low cost.

ACKNOWLEDGEMENT

This work was partly supported by Grant-in-Aid for Scientific Research (Kaken S, 24226017) and received help in the experiments from Senju Metal Industry Co. Ltd. in Japan.

REFERENCES

1. F. Roccaforte, P. Fiorenza, G. Greco, M. Vivona, R.L. Nigro, F. Giannazzo, A. Patti, and M. Saggio, *Appl. Surf. Sci.* 301, 9 (2014).
2. K. Suganuma, S. Sakamoto, N. Kagami, D. Wakuda, K.S. Kim, and M. Nogi, *Microelectron. Reliab.* 52, 375 (2012).
3. H.S. Chin, K.Y. Cheong, and A.B. Ismail, *Metall. Mater. Trans. B* 41, 824 (2010).
4. V.R. Manikam and K.Y. Cheong, *IEEE Trans. Compon. Packag. Manuf. Technol.* 1, 457 (2011).
5. T. Wang, X. Chen, G.Q. Lu, and G.Y. Lei, *J. Electron. Mater.* 36, 1333 (2007).
6. S. Sakamoto, S. Nagao, and K. Suganuma, *J. Mater. Sci. Mater. Electron.* 24, 2593 (2013).
7. Y. Morisada, T. Nagaoka, M. Fukusumi, Y. Kashiwagi, M. Yamamoto, M. Nakamoto, H. Kakiuchi, and Y. Yoshida, *J. Electron. Mater.* 40, 2398 (2011).
8. R. Khazaka, L. Mendizabal, and D. Henry, *J. Electron. Mater.* 43, 2459 (2014).
9. A.R. Rathmell, S.M. Bergin, Y.L. Hua, Z.Y. Li, and B.J. Wiley, *Adv. Mater.* 22, 3558 (2010).
10. S. Bhanushali, P. Ghosh, A. Ganesh, and W. Cheng, *Small* 11, 1232 (2015).
11. X. Liu and H. Nishikawa, *Scrip. Mater.* 120, 80 (2016).
12. H. Nishikawa, T. Hirano, T. Takemoto, and N. Terada, *Open Surf. Sci. J.* 3, 60 (2011).
13. T. Ishizaki and R. Watanabe, *J. Mater. Chem.* 22, 25198 (2012).
14. S. Jeong, S.H. Lee, Y. Jo, S.S. Lee, Y.H. Seo, B.W. Ahn, G. Kim, G.E. Jang, J.U. Park, and B.H. Ryu, *J. Mater. Chem. C* 1, 2704 (2014).
15. S.W. Park, R. Uwataki, S. Nagao, T. Sugahara, Y. Katoh, H. Ishino, K. Sugiura, K. Tsuruta, and K. Suganuma, in *Electronic Components and Technology Conference (ECTC), 2014 IEEE 64th*, (2014), pp. 1179–1182.
16. S. Soichi and K. Suganuma, *IEEE Trans. Compon. Packag. Manuf. Technol.* 3, 923 (2013).
17. J. Jiu, K. Murai, K. Kim, and K. Suganuma, *J. Mater. Sci. Mater. Electron.* 21, 713 (2010).
18. J. McCoppin, T.L. Reitz, R. Miller, H. Vijwani, S. Mukhopadhyay, and D. Young, *J. Electron. Mater.* 43, 3379 (2014).
19. S.J. Joo, H.J. Hwang, and H.S. Kim, *Nanotechnology* 25, 265601 (2014).
20. S.K. Tam, K.Y. Fung, and K.M. Ng, *J. Mater. Sci.* 51, 1914 (2016).
21. J. Jiu, H. Zhang, S. Nagao, T. Sugahara, N. Kagami, Y. Suzuki, Y. Akai, and K. Suganuma, *J. Mater. Sci.* 51, 3422 (2016).
22. Y. Li, K. Moon, H. Li, and C.P. Wong, in *Electronic Components and Technology Conference, 2004. Proceedings. 54th*, (2004), pp. 1959–1964.
23. C.A. Lu, P. Lin, H.C. Lin, and S.F. Wang, *Jpn. J. Appl. Phys.* 46, 251 (2007).
24. I. Kim and S. Chun, *J. Electron. Mater.* 40, 1977 (2011).
25. T. Ogura, S. Takata, M. Takahashi, and A. Hirose, *Mater. Trans.* 56, 1030 (2015).
26. T. Ogura, T. Yagishita, S. Takata, T. Fujimoto, and A. Hirose, *Mater. Trans.* 54, 860 (2013).
27. Y. Gao, H. Zhang, J. Jiu, S. Nagao, T. Sugahara, and K. Suganuma, *RSC Adv.* 5, 90202 (2016).
28. J.L.C. Huaman, K. Sato, S. Kurita, T. Matsumoto, and B. Jeyadevan, *J. Mater. Chem.* 21, 7062 (2011).
29. B.K. Park, S. Jeong, D. Kim, J. Moon, S. Lim, J.S. Kim, and J. Colloid, *Interface Sci.* 311, 417 (2007).